Intrahelical Arrangement in the Integral Membrane Protein Rhodopsin Investigated by Site-Specific Chemical Cleavage and Mass Spectrometry†

Andrew Gelasco,‡ Rosalie K. Crouch,§ and Daniel R. Knapp*,‡

Departments of Cell and Molecular Pharmacology and Experimental Therapeutics and Ophthalmology, Medical University of South Carolina, Charleston, South Carolina 29425

Received November 29, 1999; Revised Manuscript Received February 3, 2000

ABSTRACT: Site-specific cleavage on the interhelical loop I on the cytoplasmic face of rhodopsin has been observed after activation of a Cu-phenanthroline tethered cleavage reagent attached on the cytoplasmic loop IV. The characterization of the reaction products by mass spectrometry, both of the membrane-bound protein and of the CNBr-cleaved peptides, allows the site of cleavage to be determined precisely. The specific cleavage of the peptide bond between Q64 and H65 on loop I leaves the N-terminal peptide (M1-Q64) intact, confirmed by MALDI-MS detection of the two N-linked glycosyl groups near the N-terminus of rhodopsin. The limited extension of the tether side chain requires a interresidue distance between the cleavage site, Q64, and the site of ligand attachment, C316, of less than 12 Å. Upon photoactivation of the receptor, no change in the cleavage pattern is observed; however, a simulated Meta II intermediate activation state indicates a much more complex cleavage pattern. The development of this cleavage method, previously used primarily as a "chemical nuclease", in combination with mass spectrometry, may provide a powerful method on membrane protein conformation studies that can be used to complement other biophysical characterizations.

Rhodopsin (*1*−*3*), the prototypical G protein[1] coupled receptor (*4*), has resisted three-dimensional structural characterization by the conventional methods of NMR and X-ray crystallography due to its size and solubility and the difficulty in obtaining suitable crystals of the integral membrane protein. It is the major protein component of rod outer segments in the retina and has been the subject of intense study for nearly 30 years. The rod cell photoreceptor is an N-terminal acetylated glycoprotein consisting of a single 348-amino acid polypeptide chain that is intrinsically associated with a phospholipid membrane. Upon irradiation, isomerization of the 11-*cis*-retinal cofactor, covalently linked and embedded in the transmembrane helices, causes structural changes at the cytoplasmic loops of the membrane protein. It is these structural perturbations that are responsible for binding and activating the G protein transducin (G_T) and initiating the visual cascade.

While a high-resolution structure of rhodopsin has not yet been obtained, a number of cryoelectron microscopy studies on two-dimensional crystals of rhodopsin have revealed significant structural information regarding the gross orientation of the protein in the membranes (*5*−*7*). These projection structures provided evidence for seven transmembrane helices and showed that at least three of the helices were tilted in the membrane. More recently, higher resolution studies (up to 5 Å resolution) have revealed more positional information about the transmembrane helices (allowing tilt angles to be estimated for all seven helices) and have allowed models of the protein to be further refined (*8, 9*). In all of these cases, no information regarding the interhelical loops could be obtained due to the low resolution of the electron crystallography data. These loops and their relative orientation are the key to activation of the G proteins coupled to this class of receptors.

To study the structural interaction of the interhelical loops, a number of spectroscopic techniques have been employed. Synthetic peptides of various sequence lengths of a number of the interhelical loops have been prepared, and their solution state structures have been studied by two-dimensional NMR (*10*−*12*). These studies have indicated that the loops may have some intrinsic secondary structure observed in the solution state (*11, 12*). These loop structures can be superimposed on the projection structures of the transmembrane helices and present reasonable structures. However, these isolated interhelical regions are, of course, tethered to the helices and are in contact with a hydrophobic membrane surface in the native state, properties that probably have a

† This work was supported by NIH Grants EY08239 and EY04939, American Heart Association Grant 99512850, and M.U.S.C. Institutional Support and Foundation to Prevent Blindness. A.G. was supported by a M.U.S.C. Institutional fellowship and NSF Grant EPS-9630167.

* To whom correspondence should be addressed. Telephone: (843) 792-5840, fax: (843) 792-2475, e-mail: knappdr@musc.edu.

‡ Department of Cell and Molecular Pharmacology and Experimental Therapeutics.

§ Department of Ophthalmology.

[1] Abbreviations: G protein, guanyl nucleotide-binding regulatory protein; NMR, nuclear magnetic resonance; CNBr, cyanogen bromide; HPLC, high-performance liquid chromatography; EDTA, ethylenediaminetetraacetic acid; OP, 5-(α-bromoacetamido)-1,10-phenanthroline; DMF, dimethylformamide; KP_I, potassium phosphate; MALDI-TOF, matrix-assisted laser desorption ionization-time-of-flight; HFIPA, hexafluoroisopropyl alcohol; TFA, trifluoroacetic acid; MeOH, methanol; EtOH, ethanol; RP-HPLC, reverse phase high-performance liquid chromatography; ESI, electrospray ionization; MS/MS, tandem mass spectrometry; LC−MS, liquid chromatography−mass spectrometry, HOAc, acetic acid.

10.1021/bi992736i CCC: $19.00
Published on Web 03/31/2000

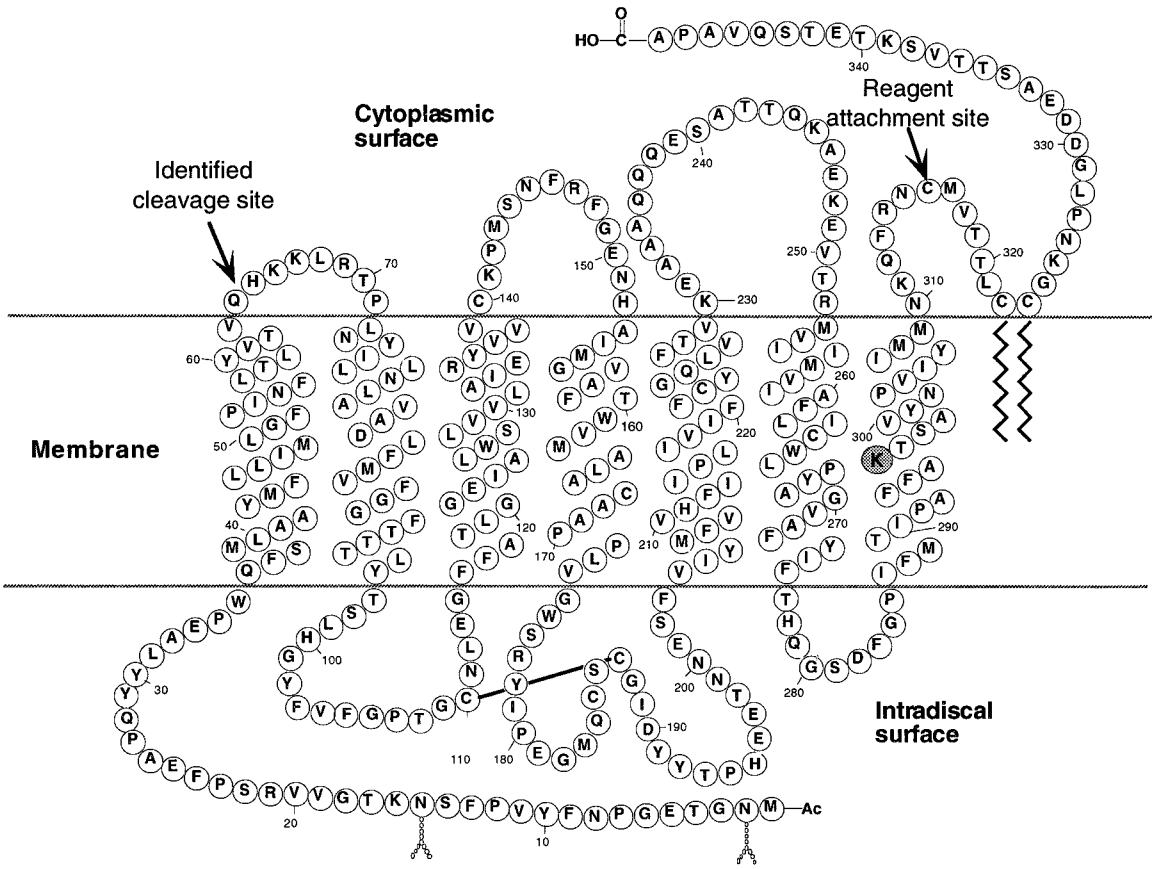

FIGURE 1: Two-dimensional diagram of rhodopsin shows the seven transmembrane helices and the location of the attached Cu ligand, OP, at C316 and the major cleavage site upon reaction with Cu/O_2/ascorbate at Q64.

significant effect on the fold of the protein. Recently, a systematic study of the solvent accessibility of a spin-label modified amino acid mutated into each position of each of the interhelical loops has been completed (*13*−*17*). These studies examined the extent of helicity extending beyond the membrane surface and addressed the issue of secondary structure of the interhelical loops. In many cases, they concluded that the NMR structures are probably not useful in determining the structure accessibility of the loops near the membrane surface, the region that is not consistent with the observed spectroscopic properties of the intact protein in detergent micelle solutions.

The present limitations on structurally characterizing membrane-bound proteins by conventional techniques have spurred interest in the use of various enzymatic and chemical cleavage techniques in combination with mass spectral analysis to identify structural and sequence features of the proteins (*18*−*21*). Previously, we have demonstrated that a systematic reduction, alkylation, delipidation, and CNBr cleavage of rhodopsin allows for the HPLC tandem mass spectrometric analysis of the entire hydrophobic protein, opening up a methodology for the study of postranslational modifications of the membrane proteins (*21*). In this study, we have used a copper reagent specifically attached to a cysteine side chain to probe the local environment of one of the interhelical loops previously proposed to undergo conformational changes upon photoactivation of rhodopsin (*22*). Figure 1 contains a two-dimensional diagram of rhodopsin showing the seven predicted transmembrane α-helices, the interhelical loops, and the site of copper reagent attachment. The use of a previously developed chemical nuclease/protease (*23*−*25*) in combination with high-resolution mass spectrometry has allowed us to determine the relative intramolecular orientation of two of the interhelical loops of rhodopsin. Through a detailed analysis of a site-specific cleavage near helix I by a Cu cleavage agent attached to the loop of helix VII, an interresidue distance of ≈10 Å has been determined.

MATERIALS AND METHODS

Materials. 3,5-Dimethoxy-4-hydroxycinnamic acid (sinapinic acid), cyanogen bromide (CNBr, 5 M in acetonitrile) (Aldrich), Tris-HCl, potassium phosphate, monobasic, sodium phosphate, dibasic (Sigma), sodium hydroxide, $CuSO_4 \cdot 5H_2O$ (Fisher), dimethylformamide (Fisher), HPLC solvents, acetonitrile and methanol (Burdick and Jackson, UV grade), 2-propanol (Fisher, Optima), and trifluoroacetic acid (J. T. Baker) were used as received without further purification. L-Ascorbic acid, reagent grade (Acros), was used to prepare solutions of sodium ascorbate adjusted to pH 6.5 with sodium hydroxide.

Trypsin, modified sequencing grade, was prepared by dissolving the lyophilized powder as received from Boehringer Mannheim in 1 mM HCl at 0.1 μg/μL. N-Glycosidase F (PNGase F) was used as obtained from Boehringer Mannheim, 25 000 units/mg in 50 mM sodium phosphate, 12.5 mM EDTA, and 50% glycerol, pH 7.2. The phenanthroline derivative, 5-(α-bromoacetamido)-1,10-phenanthroline (OP), was prepared from 5-nitro-1,10-phenanthroline (Aldrich) according to a previously published procedure (*26*), recrystallized, and characterized by ^{1}H NMR and ESI-MS.

Rod outer segments were prepared from intact bovine retina (Lawson Co., Lincoln, NE) as described previously (*27*). Membrane preparations were further purified with a 5 M urea wash to remove rhodopsin-associated proteins (*28*), leaving a suspension of nearly pure membrane-bound rhodopsin. Suspensions of the intact membrane preparations were stored at −80 °C in the dark. All subsequent manipulations were conducted under dim red light or in total darkness, until cleavage reagents were removed from the suspension or reactions were quenched.

Cu-Based Cleavage of Intact Rhodopsin. Urea-washed membrane preparations (typically 0.25 mg, 6 nmol of rhodopsin) were resuspended in a KP_I buffer (50 mM KP_I and 150 mM NaCl, pH 7.4) to a concentration of 2 mg/mL. The reagent OP was dissolved in DMF and added to the rhodopsin suspension in a 10-fold molar excess, keeping the total DMF concentration to less than 10%. The reaction was allowed to proceed for 8 h, carefully maintained at 4 °C. OP-modified rhodopsin was isolated by centrifugation (80000*g*, 20 min, and 4 °C), washed, and resuspended in KP_I buffer. $CuSO_4$ was added (1.2 equiv), and the mixture was incubated at room temperature for 15 min. The solution was made 100 mM in sodium ascorbate (adjusted to pH 6.5), and the mixture was incubated at 37 °C for 30 min. The cleavage reaction was quenched by the addition of 5 mM neocuproine, the cleaved rhodopsin isolated by centrifugation, and the pellet washed three times with dH_2O.

MALDI Mass Spectrometry. MALDI mass spectrometry was conducted on a Perseptive Biosystems Voyager-DE MALDI-TOF instrument. Samples of the integral membrane products were prepared for MALDI-MS by a modification of a published method (*29*). The sample, dissolved in formic acid:H_2O:HFIPA 7:3:2, was diluted 3:1 with 50 mM sinapinic acid in 70% acetonitrile and 0.1% TFA. The MALDI sample was prepared by addition of 0.6 μL of the matrix solution to the plate that was allowed to dry, and then 0.6 μL of sample/matrix mixture was placed on the dried matrix surface. This preparation gave significant improvement over the previously published procedure in signal/noise and, to a lesser extent, improvement in peak resolution. Samples of peptide fragments were prepared by dilution in 50 mM α-cyano-4-hydroxycinnamic acid in 50% MeOH and 0.1% TFA, which was applied directly to the MALDI sample plate.

HPLC-ESI Mass Spectrometry. Membrane-bound fragments were reduced with tributylphosphine and alkylated with 4-vinyl pyridine as previously described (*21*). The rhodopsin membrane was then disrupted by addition of 500 μL of EtOH and 300 μL of hexane for 1 h. Solvents were removed by use of a Speedvac concentrator. The dried pellet was then subjected to either a trypsin (1.5 μg of trypsin in HCl in 25 mM NH_4HCO_3, 0.1% *n*-octyl glucoside, pH 8) or a CNBr (in 70% TFA) digest. The digest product was dissolved in 5 μL of TFA, and then acetonitrile, 2-propanol, and water were added to give a final solution equivalent to the initial RP-HPLC mobile phase of 98% aqueous/2% 2:1 2-propanol:acetonitrile.

The digest samples were loaded onto a Aquapore OD-300 (Brownlee) RP-C18 2.1 × 100 mm column at 200 μL/min using a Hewlett-Packard model 1100 HPLC system equipped with a 2-mL injection loop at 200 μL/min for 12 min. The peptides were separated by using a mobile phase gradient of 98% A (0.05% aqueous TFA)/2% B (2:1 2-propanol:acetonitrile, 0.043% TFA) to 40% A/60% B in 60 min, followed by a gradient to 2% A/98% B in 20 min.

The column effluent was split 10:1 with approximately 20 μL/min flowing to the ESI source of a Finnigan LCQ ion trap mass spectrometer. Instrument parameters were set as follows: ESI voltage, 4.5 kV; capillary voltage, 46 V; capillary temperature, 200 °C; MS scan range, 300−2000 amu; isolation width, 2 amu; MS/MS collision energy, 45%. The instrument was run, and data were collected under control of the LCQ Xcalibur software suite (Thermoquest) and analyzed with the Qual Browser package. MS/MS data were collected continuously on the most intense peak in each mass spectrum. Dynamic exclusion was set for a repeat of 3/30 s to exclude the peak for 3 min.

Nanospray MS/MS. Low-flow electrospray was carried out on a home-built nanospray platform equipped with glass capillaries (1 mm i.d. borosilicate; Kimble 46485) pulled to a fine needle tip (1−5 μm) with a Sutter Instruments Co. model P-2000 tube puller. Spray parameters were identical to those for ESI except as follows: ESI voltage, 1.1 kV; MS scan range, 150−2000. Samples were typically prepared from 200 μL HPLC fractions by removing the eluent in vacuo and dissolving the peptides in 5−10 μL of 47/47/6 MeOH/H_2O/HOAc solvent mixture. Approximately 1−2 μL of the mixture was loaded into a glass tip by capillary action that provided 5−15 min of sprayed sample. MS/MS data were collected in manual mode through the Xcalibur LCQ Tune software.

RESULTS

Labeling Cys316 with 5-(α-Bromoacetamido)-1,10-phenanthroline. Previous studies on the solvent accessibility of rhodopsin have indicated that only 2 of the 10 cysteines in the protein are reactive toward various labeling procedures. Following from the observations of Yeagle et al. (*30*), the membranes were incubated at 4 °C with the phenanthroline derivative OP, which causes modification of primarily C316. Following incubation and precipitation, the modified protein was characterized by both MALDI-MS and HPLC-ESI-MS/MS.

Matrix-assisted laser desorption ionization-mass spectrometry (MALDI-MS) requires the mixing of a solution of an organic matrix that absorbs at the laser wavelength (commonly a cinnamic acid derivative for ultraviolet lasers) with a solution of the peptide or protein to be analyzed. The protein/matrix mixture is then spotted and allow to dry on a sample probe or plate that can be inserted in the vacuum chamber of the mass spectrometer. Protonated ions are generated by a pulsed laser beam directed onto the protein/matrix spot. This type of ionization generally produces singly charged intact molecular ions (i.e., with little or no fragmentation), and the mass-to-charge ratio (*m*/*z*) measured, typically by a time-of-flight analyzer, then represents the molecular mass of the peptide.

Electrospray ionization mass spectrometry (ESI-MS) uses a needle tip maintained at a high electrical potential to generate a fine spray of charged droplets that are subsequently desolvated to yield a series of multiply protonated and therefore multiply charged ions for peptide and protein molecules. The *m*/*z* values measured for the various multiply

charged ions (i.e., with different charge states) can be deconvoluted to obtain the molecular mass of the peptide or protein. Ions generated by ESI-MS can also be analyzed by tandem mass spectrometry (MS/MS) in which a first stage of mass spectrometry is used to select an ion of interest, which is then fragmented through collision with a inert gas. The fragments generated from peptide ions are predominantly those formed by cleavage along the backbone peptide bonds. These fragments give a mass spectrum that can contain peaks separated by masses corresponding to the various amino acid residues, allowing determination of the sequence of the peptide. Modified residues are characterized by appropriate mass shifts in the residue masses, that is, a modified residue yields a larger mass separation between the backbone ion masses.

MALDI-MS has been demonstrated to be applicable to characterization of the integral membrane proteins and in particular to rhodopsin (*29*). Rhodopsin contains two different sites of glycosylation near the N-terminus at N2 and N15. The MALDI mass spectrum does not present the mass for a single peptide but rather a broad peak representing the major glycosylated peptide and a series of shoulders due to the presence of other glycosyl side chains. This broad peak shape presents limits on the use of MALDI-MS as a method of identifying ligand attachment. However, when MALDI mass spectra were obtained on samples of unmodified rhodopsin and ligand-modified rhodopsin run under identical conditions, a shift of *m*/*z* 200−250 was consistently observed.

We were able to use MALDI-MS experiments to demonstrate the effectiveness of low temperature on site-specific modification as well. When rhodopsin was allowed to react with excess OP ligand at 23 °C instead of 4 °C, the broad peak representing the intact protein was broadened further appearing as two shoulders, with its average *m*/*z* value increased *m*/*z* 500−600 over the unmodified protein. This observation is consistent with the reactivity predicted for the cytoplasmic sulfhydryls C140 and C316 (*30*, *31*).

Confirmation of both the extent and the position of modification by OP was obtained through HPLC-MS/MS and MALDI-MS on CNBr-cleaved OP-modified rhodopsin. MALDI mass spectra of the peptide mixture resulting from reduction/alkylation, delipidation, and CNBr cleavage of both unmodified and OP-modified rhodopsin indicated that 90−100% of C316 was converted to the 1,10-phenanthroline derivative (C316OP) and that 80−90% of C140 was converted to the 4-vinylpyridyl derivative. HPLC-ESI-MS/MS confirmed the observation of nearly quantitative conversion of C316 to C316OP and confirmed the position of modification through the fragmentation pattern of the CNBr peptide N310-M317. The selected ion chromatograms for the C316OP peptide and C316 peptide are shown for a typical HPLC-ESI-MS run in supplemental Figure 1. The MS/MS spectrum for the C316OP peptide is shown in supplemental Figure 2.

Single-Site Cu/O_2 Cleavage of Rhodopsin. The cleavage reaction following generation of the Cu−OP complex on C316 was performed as described in the Materials and Methods section. The cleavage products were isolated by centrifugation, washed, and subjected to MALDI-MS analysis. A MALDI spectrum of C316OP rhodopsin before and after cleavage is shown in Figure 2. As controls, unmodified C316 rhodopsin was incubated with Cu and ascorbate, and

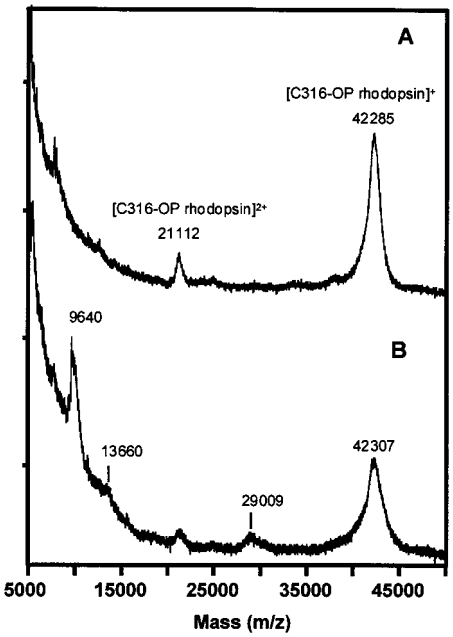

FIGURE 2: MALDI-MS of C316OP-rhodopsin before (A) and after (B) cleavage by Cu/O_2/ascorbate for 20 min.

C316OP rhodopsin was incubated in ascorbate in the absence of Cu. For both controls, the MALDI spectra were indistinguishable before and after incubation. As shown in Figure 2, there are two major products detected by MALDI after the cleavage reaction, intact rhodopsin, and the major peak at *m*/*z* 9640. Broad peaks having masses between 10 and 30 kDa were observed under various conditions, but with none of the intensity of either the *m*/*z* 9640 or 42307 peaks.

The shape of the *m*/*z* 9640 peak was consistent with inhomogeneous glycosylation and suggested that the corresponding fragment peptide contained the N-terminus of the protein. If the N-terminus is otherwise uncleaved, the cleavage site due to the Cu/O_2 reaction can be predicted using the peptide sequence and the most common glycosylation oligosaccharide. The three closest sequences based on these criteria are M1-V63 (9468.4 Da), M1-Q64 (9596.7 Da), and M1-H65 (9733.8 Da). Additional evidence for the position of cleavage was obtained after reaction of the cleavage products with N-glycosidase F, which specifically removes N-linked glycosyl groups. Analysis by MALDI of the postreaction products resulted in a shift of the peak observed at *m*/*z* 9640 to *m*/*z* 7434 determined after internal calibration with insulin (5734.6) and thioredoxin (11674.5), as shown in Figure 3. This mass shift is consistent with the loss of the two N-linked glycosyl groups on N2 and N15 and conversion of the asparagine to aspartic acid at these positions. The resulting MALDI peaks were significantly less broad, allowing a more accurate mass measurement. The observed mass of the deglycosylated fragment was closest to that predicted for the M1-Q64 peptide; however, this mass is 29 Da too high. This mass difference can be accounted for, within experimental error, with two side-chain oxidations on the peptide.

Two possible sites of oxidation are found in the M1-Q64 peptide: M1, which can be oxidized to the sulfoxide or the sulfone, and W35, which can be oxidized at the 2 position on the indole ring. These potential oxidation sites were investigated through LC-MS. The Cu/O_2-cleaved, deglyco-

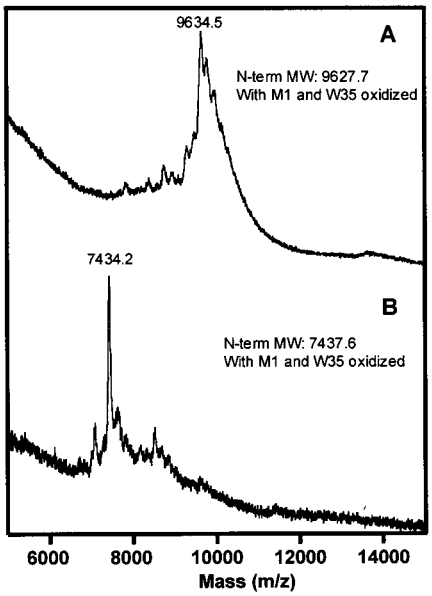

FIGURE 3: MALDI-MS of the major C316OP Cu/O_2/ascorbate cleavage product of rhodopsin before (A) and after (B) reaction with N-glycosylase F. The mass shift is consistent with the loss of 2 equiv of the major N-glycosyl product. The mass for the major peak in panel B corresponds to the calculated mass of the peptide M1-Q64 with N-terminal acetylation and oxidation of the M1 and W35 side chains.

sylated rhodopsin mixture was delipidated as previously described. The resulting pellet was dissolved in NH_4HCO_3 buffer and subjected to trypsin cleavage. The solvent was removed in vacuo after addition of TFA to 10% v/v, and the resulting material was dissolved in the initial mobile phase of the gradient and analyzed by HPLC-ESI-MS. The tryptic peptide M1-K16 was detected in both the native state and in the singly oxidized form separated by 2 min by HPLC. The chromatogram and corresponding mass spectra are shown in supplemental Figure 3. The M1-sulfoxide-containing peptide was found in a 2:1 excess over the unmodified peptide. No sulfone-containing peptide was detected under the conditions of the experiment. The detection of oxidation at W35 was less conclusive, primarily due to the large size of the peptide containing the oxidized tryptophan, but could be observed. Oxidation at these two sites would result in a peptide with a mass of 7437 that is within 2.5 Da of the MALDI peak detected.

Identification of the Cu/O_2 Cleavage Site. The site of cleavage was confirmed by HPLC-ESI-MS/MS of the CNBr cleavage products of the Cu/O_2-cleaved protein. The protein was delipidated as described for the trypsin digest and then subjected to CNBr digestion. CNBr cleavage of rhodopsin yields 17 peptides (fragments 1−17 numbered from the N-terminus), and Cu/O_2 cleavage at Q64 would be a cut in fragment 5. Omission of the reduction and alkylation step prior to delipidation and CNBr cleavage made detection of all of the rhodopsin peptides impossible, but fragments 3 and 4 from the N-terminus and fragment 14 from helix VII were observed and used as internal standards. The resulting HPLC-MS analysis showed a significant loss of the intact CNBr peptide 5 (L50-M86) and the appearance of two peptides corresponding in mass to two cleaved products of the 36 amino acid fragment. Figure 4 shows the selected ion chromatograms for the CNBr peptides of the N-terminus cleavage product. Quantitation of the disappearance of fragment 5, the largest peak in the control chromatogram, indicates a loss of over 95%. Figure 4 also contains the selected ion chromatograms and corresponding mass spectra for the two fragments resulting from the Cu/O_2 cleavage of

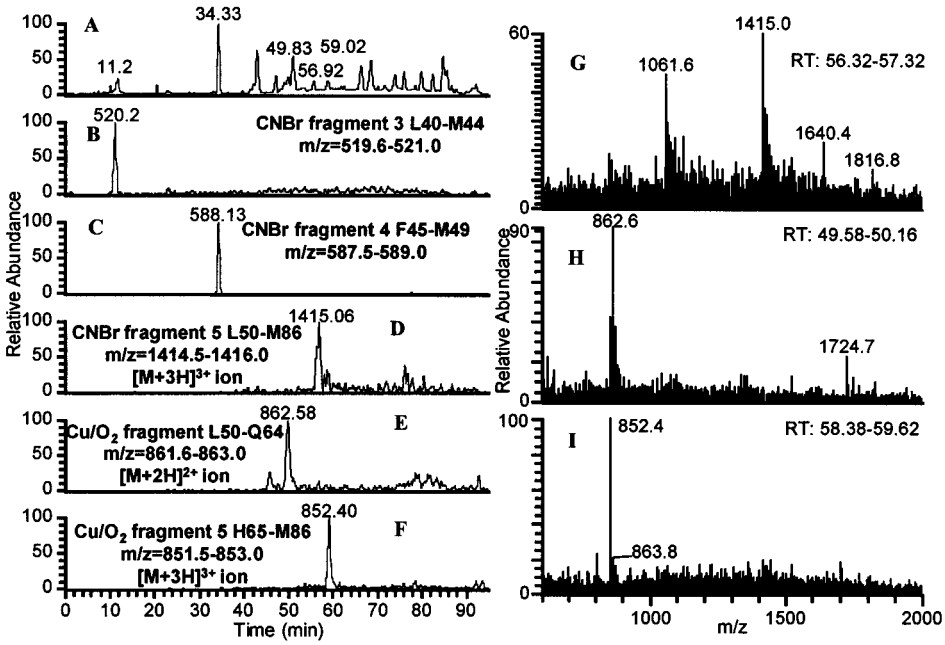

FIGURE 4: Total ion chromatogram, selected ion chromatograms (SIC), and corresponding mass spectra for the observed CNBr cleavage products of the C316OP Cu/O_2/ascorbate cleavage products of rhodopsin. Chromatogram A shows the total ion chromatogram for the HPLC-ESI-MS run on the Cu/O_2/ascorbate-cleaved, delipidated, CNBr-cleaved rhodopsin products. Chromatograms B, C, and D show the SIC for CNBr fragments 3 (L40-M44), 4 (F45-M49), and 5 (L50-M86). As described in the text, the quantity of fragment 5 is greatly diminished, and the two peptides produced by C316OP Cu/O_2/ascorbate and CNBr cleavage are observed. Chromatograms E and F represent the peptides L50-Q64 and H65-M86, respectively. MS in G ($[M + 4H]^{4+}$, *m/z* 1061.6 and $[M + 3H]^{3+}$, *m/z* 1415.0 ions), H ($[M + 2H]^{2+}$, *m/z* 862.6 and $[M + H]^{+}$, *m/z* 1724.7 ions) and I ($[M + 3H]^{3+}$, *m/z* 852.4 ion) correspond to the peptides detected in chromatograms D, E, and F, respectively.

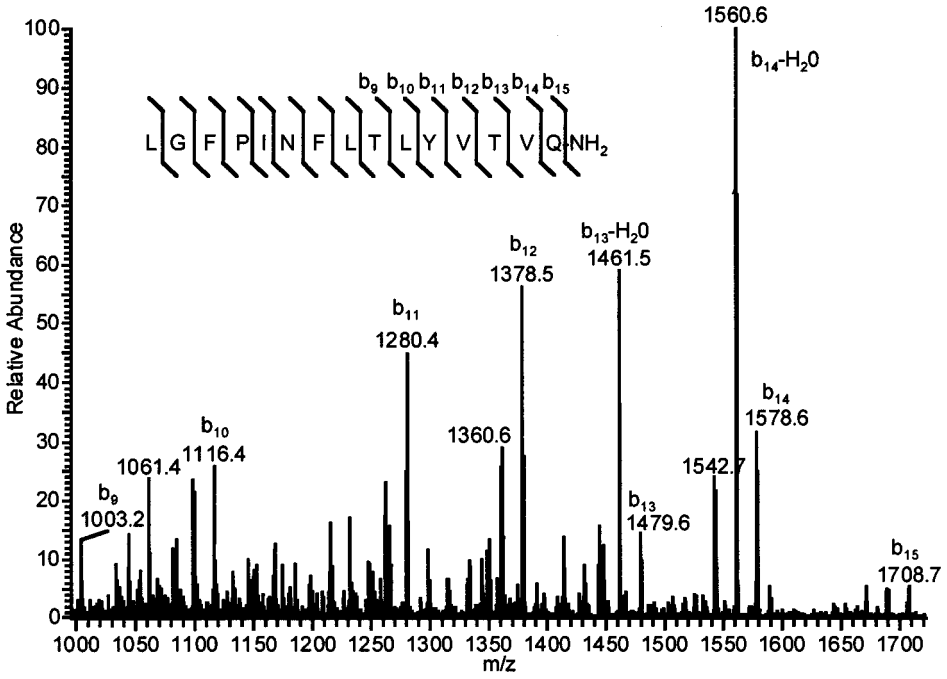

FIGURE 5: Tandem mass spectrum obtained for the CNBr peptide L50-Q64 using nanospray MS/MS. The b series from b_9 to b_{15} is shown, fragmented from the *m*/*z* 1724.7 parent ion.

the CNBr peptide fragment 5. The observed mass-to-charge ratio (*m*/*z*) for each fragment was consistent with cleavage at Q64. The N-terminal side of the fragment peptide L50-Q64 was easily detected by ESI-MS as both the singly and the doubly charged peptide containing a C-terminal amide (Figure 4B) with *m*/*z* values of 862.58 and 1724.7, respectively. This observation was consistent with a previously proposed mechanism for the cleavage of peptide bonds using the Cu/O_2 phenanthroline reagent, in which the nitrogen from the N-terminal amino acid residue of the C-terminal fragment is retained as a C-terminal amide on the N-terminal fragment (*32*, *33*).

Studying the reaction products of rhodopsin by mass spectrometry allows the mechanism of the cleavage reaction to be investigated by obtaining accurate mass measurements of the resulting peptides. For the N-terminus, the amide transfer results in only a 1 amu mass shift in the resulting peptide. This shift is observed in both the MS and the MS/MS patterns for the peptide. The nanospray tandem MS of the N-terminal peptide confirmed its identity through the b series (*34*) of peptide fragments (b_9-b_{15}) and is shown in Figure 5. The C-terminal end of the cleaved CNBr peptide (H65-M86) has a predicted mass of 2537.04 for a peptide containing the homoserine lactone C-terminus and the ketoacyl group on the N-terminus resulting from amide donation to Q64. This peptide has masses corresponding to the $[M + 2H]^{2+}$ and $[M + 3H]^{3+}$ ions of 1269.03 and 846.65, respectively. No measurable amounts of these peptides were detected but rather a peak eluting 10 min after the L50-Q64 peptide with a *m*/*z* of 852.38. This mass spectrum corresponded to that of the $[M + 3H]^{3+}$ ion for an oxidation product of the parent peptide or the hydrolyzed lactone C-terminus. Unfortunately, this fragment did not lend itself to MS/MS analysis, and additional information regarding this modification was not obtained. However, previous work with model peptides (*35*) suggests that oxidation of the N-terminal histidine residue side chain of the H65-M86 cleavage fragment to the 2-oxo derivative is the probable cause of the observed mass shift for the fragment ion.

DISCUSSION

The lack of a high-resolution structure of rhodopsin and, specifically, structural information regarding the cytoplasmic interhelical loops requires that various indirect chemical and spectroscopic techniques be applied toward the investigation of intramolecular and intermolecular interactions of rhodopsin. Kaback and co-workers utilized oxidative cleavage catalyzed by a copper ion bound to OP, in conjunction with gel electrophoresis analysis, to probe the structure of another integral membrane protein, lactose permease (*25*). We have used mass spectrometry to extend the application of the technique to rhodopsin. The use of mass spectrometry allows the details of the cleavage site to be investigated more precisely than by the use of electrophoretic analysis. This technique also has the potential to be used to monitor the changes of receptor binding sites upon activation and to investigate recognition sites in protein−protein interactions.

The presence of two different reactive sulfhydryl groups on the cytoplasmic surface of rhodopsin required that all manipulations of the protein be carried out at 4 °C to direct OP modification to only Cys 316 of loop 4 (Figure 1) (*30*). MALDI-MS of the intact protein allowed us to follow the reaction by observing the mass shift versus the control protein after addition of excess OP. The specificity of C316 labeling and the exclusion of the OP label at C140 were confirmed by MALDI and ESI-MS of the CNBr cleavage fragments of the modified protein.

Having control over the localization of the single cleavage agent is important in this case because we are interested in using this probe in native, intact, membrane-bound rhodopsin. These criteria would prevent us from using known expression and isolation schemes for rhodopsin mutants in COS-1 cells resuspended in detergent micelles (*36*, *37*). Once the single

ligand site was confirmed, Cu (as $CuSO_4$) and ascorbate were added in the dark to initiate the cleavage reaction. Initially, we chose conditions that caused incomplete cleavage of rhodopsin. The reaction was monitored primarily through MALDI-MS and the appearance of a peak at *m*/*z* 9640. When the reaction was run for 5−10 min, in addition to the new peak at *m*/*z* 9640, a significant peak remained in the MALDI spectrum for the intact protein at *m*/*z* 42 000. This observation was consistent with SDS−PAGE analysis of the reaction mixtures in which the strongest band was observed for intact rhodopsin and a broad, less intense band appeared below 10 kDa. Allowing the cleavage reaction to go up to 40 min caused almost complete loss of the 42 kDa peak and an increase in the peak at 9.6 kDa. No other significant peaks were observed in the MALDI spectrum of these cleavage reactions at *m*/*z* ranges above 10 kDa.

By using the 40 min reaction time, we were able to obtain the highest concentration of the major 9.6 kDa product and to proceed with characterizing the specific cleavage site by ESI-MS and MS/MS. Initially, the reaction mixture was prepared for CNBr cleavage by the method that we had previously established (*21*). However, this methodology involves the precipitation of the pellet after each step, and the 9.6 kDa product was being lost, as measured by subsequent MALDI spectra, during these steps of alkylation/reduction and delipidation. As an alternative, we left out the reduction/alkylation step; doing so causes peptides with unblocked cysteines to be undetectable by HPLC-MS, but this is not a problem for the first five CNBr fragments. The delipidation step was modified so that the EtOH/hexane mixture was used to disrupt the lipid bilayer, but then the solvents were removed in vacuo leaving a dried mixture of lipid and peptide. This delipidation method works for intact rhodopsin as well; the peptide chromatogram is identical to that obtained using the standard delipidation procedure. The CNBr peptides are well-separated on the reverse-phase column from the phospholipids, which elute from the column in 98% organic phase.

Figure 4D shows the selected ion chromatogram for the CNBr fragment 5, which contains the identified site of cleavage by the Cu(OP) reagent attached at C316. We were able to obtain HPLC-MS data for the same sample of C316OP-rhodopsin before and after Cu/O_2 cleavage. In the chromatograms shown in Figure 4, the signal from the intact fragment 5 is greatly diminished from the control following cleavage. The presence of the two other peptides observed in the N-terminal peptide that are retained after Cu/O_2 cleavage allows us to quantitate the loss of fragment 5 by comparison to these fragments (3 and 4) as internal standards. In this case, the quantity of fragment 5 is less than 5% that of the control. As shown in Figure 4E,F, we were able to separate by HPLC and detect by MS the two peptides that result from CNBr cleavage of the Cu/O_2 cleavage products. These are previously undetected peptides, so no standard means of quantitating them versus the loss of the parent fragment is possible.

We were able to further confirm the specific site of cleavage by obtaining MS/MS data on the N-terminal cleavage fragment of CNBr fragment 5. While MS/MS data were collected during the LC-MS run, more complete data were obtained by nanospray MS/MS. A representative spectrum is shown in Figure 5. These data confirm both the site of the cleavage on the first interhelical loop and the amide transfer from H65 to the C-terminus of Q64.

This tethered chemical protease technique has now been demonstrated to work well in two different membrane proteins to give a specific and reproducible cleavage pattern. The introduction of mass spectrometric analysis of the cleavage products has greatly enhanced applicability of the technique because specific cleavage sites, patterns, and mechanisms can be investigated with a high level of precision. In the case of the G protein-coupled receptors, this kind of reagent has great potential to be applied toward investigating protein−protein interactions. This type of methodology is complemented by other spectroscopic techniques such as site-directed spin labeling of proteins demonstrated recently (*38*). As described by Kaback and coworkers (*25*), however, these tethered cleavage reagents have the advantage of being applied in the native state and therefore can be used to examine these native state conformations as we have demonstrated.

In addition to examining protein−protein interactions, in the case of the receptor itself, this technique has the potential of being able to probe conformational changes of the protein surfaces upon activation. While this study has focused on developing the use of the Cu/O_2/OP protease in combination with mass spectrometry, it should be applicable to examine potentially the structural changes on the cytoplasmic surface of rhodopsin upon photoactivation and then to probe the binding surface of G_T.

Preliminary work on the photoactivated state of rhodopsin has produced interesting observations. While photobleaching the chromophore resulted in no significant change in the cleavage pattern of the protein, reactivation of the receptor with an 11-*cis*-retinal analogue β-ionone, a mimic for the Meta II intermediate (*39*, *40*), causes a more complex cleavage pattern to appear. We are currently investigating this result since, unfortunately, the conditions previously reported to be necessary to trap the Meta II intermediate require very low pH, a condition that inhibits the Cu/O_2/OP cleavage.

ACKNOWLEDGMENT

We thank Ms. Brandi Newsome for rhodopsin preparations and Drs. Kevin Schey and John Oatis for helpful discussions.

SUPPORTING INFORMATION AVAILABLE

Supporting Information is available including additional mass spectral data as described in the text (supplemental Figures 1−3; 4 pages). This material is available free of charge via the Internet at http://pubs.acs.org.

REFERENCES

1. Khorana, H. G. (1992) *J. Biol. Chem. 267*, 1−4.
2. Hargrave, P. A., and McDowell, J. H. (1992) *FASEB J. 6*, 2323−2331.
3. Sakmar, T. P. (1998) *Prog. Nucleic Acids Res. Mol. Biol. 59*, 1−34.
4. Baldwin, J. M. (1994) *Curr. Opin. Cell Biol. 6*, 180−190.
5. Schertler, G. F. X., Villa, C., and Henderson, R. (1993) *Nature 362*, 770−772.
6. Unger, V. M., and Schertler, G. F. X. (1995) *Biophys. J. 68*, 1776−1786.
7. Schertler, G. F. X., and Hargrave, P. A. (1995) *Proc. Natl. Acad. Sci. U.S.A. 92*, 11578−11582.

8. Unger, V. M., Hargrave, P. A., Baldwin, J. M., and Schertler, G. F. X. (1997) *Nature 389*, 203−206.
9. Krebs, A., Villa, C., Edwards, P., and Schertler, G. (1998) *J. Mol. Biol. 282*, 991−1003.
10. Yeagle, P. L., Alderfer, J. L., and Albert, A. D. (1995) *Nat. Struct. Biol. 2*, 832−834.
11. Yeagle, P. L., Alderfer, J. L., and Albert, A. D. (1995) *Biochemistry 34*, 14621−14625.
12. Yeagle, P. L., Alderfer, J. L., Salloum, A. C., Ali, L., and Albert, A. D. (1997) *Biochemistry 36*, 3864−3869.
13. Farahbakhsh, Z., Ridge, K., Khorana, H., and Hubbell, W. (1995) *Biochemistry 34*, 8812−8819.
14. Altenbach, C., Yang, K., Farrens, D. L., Farahbakhsh, Z. T., Khorana, H. G., and Hubbell, W. L. (1996) *Biochemistry 35*, 12470−12478.
15. Altenbach, C., Klein-Seetharaman, J., Hwa, J., Khorana, H. G., and Hubbell, W. L. (1999) *Biochemistry 38*, 7945−7949.
16. Altenbach, C., Cai, K., Khorana, H. G., and Hubbell, W. L. (1999) *Biochemistry 38*, 7931−7937.
17. Langen, R., Cai, K., Altenbach, C., Khorana, H. G., and Hubbell, W. L. (1999) *Biochemistry 38*, 7918−7924.
18. Orlando, R., Kenny, P. T. M., Moquin-Pattey, C., Lerro, K. A., and Nakanishi, K. (1993) *Org. Mass Spectrom. 28*, 1−8.
19. Papac, D. I., Oatis, J. E., Crouch, R. K., and Knapp, D. R. (1993) *Biochemistry 32*, 5930−5934.
20. Barnidge, D. R., Dratz, E. A., Sunner, J., and Jesaitis, A. J. (1997) *Protein Sci. 6*, 816−824.
21. Ball, L. E., Oatis, J. E., Dharmasiri, K., Busman, M., Wang, J., Cowden, L., Galijatovic, A., Chen, N., Crouch, R. K., and Knapp, D. R. (1998) *Protein Sci. 7*, 758−764.
22. Resek, J., Farahbakhsh, Z. T., Hubbell, W. L., and Khorana, H. G. (1993) *Biochemistry 32*, 12025−12032.
23. Sigman, D. S., Kuwabara, M. D., Chen, C.-H. B., and Bruice, T. W. (1993) *Methods Enzymol. 208*, 414−425.
24. Sigman, D. S., Mazumder, A., and Perrin, D. A. (1993) *Chem. Rev. 93*, 2295−2316.
25. Wu, J., Perrin, D. M., Sigman, D. S., and Kaback, H. R. (1995) *Proc. Natl. Acad. Sci. U.S.A. 92*, 9186−9190.
26. Perrin, D. M., Mazumder, A., Sadeghi, F., and Sigman, D. S. (1994) *Biochemistry 33*, 3848−3854.
27. McDowell, J. H., and Kuhn, H. (1977) *Biochemistry 16*, 4054−4060.
28. Shichi, H., and Somers, R. L. (1978) *J. Biol. Chem. 253*, 7040−7046.
29. Schey, K. L., Papac, D. I., Knapp, D. R., and Crouch, R. K. (1992) *Biophys. J. 63*.
30. Albert, A. D., Watts, A., Spooner, P., Groebner, G., Young, J., and Yeagle, P. L. (1997) *Biochim. Biophys. Acta 1328*, 74−82.
31. Chen, Y. S., and Hubbell, W. L. (1978) *Membr. Biochem. 1*, 107−130.
32. Bateman, R. C., Jr., Youngblood, W. W., Busby, W. H., Jr., and Kizer, J. S. (1985) *J. Biol. Chem. 260*, 9088−9091.
33. Bradbary, A. F., and Smith, D. G. (1991) *Trends Biochem. Sci. 16*, 112−114.
34. Biemann, K. (1990) *Methods Enzymol. 193*, 886−887.
35. Khossravi, M., and Borchardt, R. T. (1998) *Pharm. Res. 15*, 1096−1102.
36. Ridge, K. D., Zhang, C., and Khorana, H. G. (1995) *Biochemistry 34*, 8804−8811.
37. Yang, K., Farrens, D. L., Hubbell, W. L., and Khorana, H. G. (1996) *Biochemistry 35*, 12464−12469.
38. Hubbell, W. L., Gross, A., Langen, R., and Lietzow, M. A. (1998) *Curr. Opin. Struct. Biol. 8*, 649−656.
39. Kefalov, V. J., Cornwall, M. C., and Crouch, R. K. (1999) *J. Physiol. (London) 113*, 491−503.
40. Buczylko, J., Saari, J., Crouch, R. K., and Palczewski, K. (1996) *J. Biol. Chem. 271*, 20621−20630.

BI992736I